Vibrational energy transfer in Ar-O_3 collisions: Comparison of rotational sudden, breathing sphere, and classical calculations

Reinhard Schinke, Mikhail Ivanov

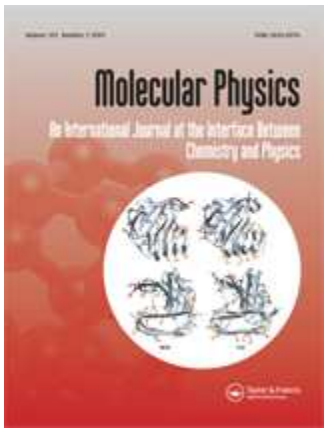

Vibrational energy transfer in Ar-O_3 collisions: Comparison of rotational sudden, breathing sphere, and classical calculations

Journal:	*Molecular Physics*
Manuscript ID:	TMPH-2009-0282.R1
Manuscript Type:	Special Issue Paper - In honour of Prof Werner 60th birthday
Date Submitted by the Author:	07-Oct-2009
Complete List of Authors:	Schinke, Reinhard; MPI-DS Ivanov, Mikhail; MPI-DS
Keywords:	ozone, energy transfer, stabilization
Note: The following files were submitted by the author for peer review, but cannot be converted to PDF. You must view these files (e.g. movies) online.	
IOS.tex	

Vibrational energy transfer in $Ar - O_3$ collisions: Comparison of rotational sudden, breathing sphere, and classical calculations

M. V. Ivanov* and R. Schinke†

Max-Planck-Institut für Dynamik und Selbstorganisation

D-37073 Göttingen, Germany

The state-specific vibrational energy transfer, ΔE_n, in collisions of excited ozone molecules with argon atoms is investigated by means of the quantum mechanical infinite order sudden approximation. Calculations are performed for the isotopomers $^{16}O^{16}O^{16}O$, $^{16}O^{18}O^{16}O$, and $^{16}O^{16}O^{18}O$. The infinite order sudden approximation yields an energy transfer which at low ozone energies exceeds the energy transfer previously obtained with the breathing sphere approximation by an order of magnitude. For energies close to the dissociation threshold, however, the mismatch is reduced to less than a factor of two. On the other hand, the rotational sudden energy transfer agrees well with the results of classical trajectory calculations over a wide range of ozone energies.

I. INTRODUCTION

The recombination of ozone shows an intriguing isotope effect[1] which, in spite of numerous theoretical efforts,[2] is not yet fully understood. The rate coefficient for the formation of non-symmetric isotopomers — for example 688 or 866, where 6 and 8 stand for ^{16}O and ^{18}O, respectively — depends linearly on the difference of zero-point energies of the possible O_2 dissociation products (Δ_{ZPE}).[3] This dependence has been explained by statistical,[4] classical trajectory,[5] and quantum mechanical[6] calculations. According to the experimental data[3] the rate coefficients for forming symmetric ozone isotopomers with $\Delta_{ZPE} = 0$ — for example 666 or 686 — do not follow the linear dependence: They are all by 15%– 20% smaller than expected from the results of the non-symmetric isotopomers. This apparent symmetry effect has not been explained up to now. Both, the association/dissociation, $O + O_2 \rightleftharpoons O_3^*$, and

* mivanov@gmx.de
† rschink@gwdg.de

the stabilization, $O_3^* + M \rightarrow O_3 + M$, can be affected by symmetry,[4,7,8] where M represents a buffer gas. The density of vibrational quantum states in asymmetric ozone is roughly twice the density of symmetric or anti-symmetric vibrational states in symmetric ozone and this difference may influence the intramolecular dynamics of ozone as well as the energy exchange with M.

In a recent study[9] (hereafter termed I) we investigated the vibrational energy transfer in collisions of O_3 with Ar using a most simple quantum mechanical approximation: the breathing sphere approximation (BSA). Within the BSA the six-dimensional $Ar - O_3$ potential energy surface (PES) is first averaged over the two $Ar - O_3$ orientation angles θ and φ. This completely eliminates rotational transitions and thus drastically simplifies the scattering calculations. An inherent feature of the BSA is that for symmetric isotopomers transitions between symmetric and anti-symmetric ozone states are strictly forbidden. The main goal in I was to test whether the collisional energy transfer, and therefore the stabilization rate, is different for symmetric and non-symmetric molecules.

The main results of I can be summarized as follows: (1) The individual cross sections for vibrationally inelastic transitions $n \rightarrow n'$ show large fluctuations as function of n'; the fluctuations reflect the nodal structures of the underlying vibrational wave functions of O_3. (2) The inelastic probabilities are sufficiently small that first-order perturbation theory can be used for analysis, even for initial states close to the dissociation threshold. (3) The energy transfer ΔE_n is a strongly fluctuating function of the initial state n and therefore substantial averaging is mandatory for comparing the results for different isotopomers. (4) The BSA calculations show a strong symmetry effect for low initial ozone states, where the energy transfer for the non-symmetric molecules is by an order of magnitude larger than for the symmetric ones. However, for higher initial states with energies E_n exceeding half of the dissociation energy, ΔE_n is almost indistinguishable for symmetric and non-symmetric molecules. (5) The results can be rationalized in terms of the polyad structure of the vibrational spectrum and several near-resonance conditions. (6) Except for the non-symmetric isotopomers in the low-energy regime, ΔE_n increases very strongly with E_n and is proportional to $(E_n - E_0)^k$ with $k = 5$–7. The main conclusion of I was that, within the BSA, the energy exchange between highly excited ozone complexes close to the dissociation threshold with the buffer gas is independent of the symmetry.

The BSA is a very crude approximation and is not expected to be *quantitatively* correct.[10]

In the present study we investigate the vibrational energy transfer in $Ar - O_3$ collisions by means of the more accurate infinite order sudden approximation (IOSA) for the rotational degrees of freedom.[11–13] Vibrationally inelastic scattering calculations are performed for fixed $Ar - O_3$ orientations (θ, φ) and the cross sections — rather than the interaction potential as in the BSA — are finally averaged over all orientations; the anisotropy of the six-dimensional PES is fully retained in the scattering calculations.[14] Averaging of the cross sections makes the IOSA calculations about two orders of magnitude more time-consuming than the BSA calculations. However, unlike in the BSA, transitions between symmetric and anti-symmetric states for symmetric molecules are allowed. The IOSA has been applied before for studying ozone recombination,[15,16] albeit in strongly limited ways.

II. CALCULATIONS

A. Quantum mechanical calculations

Calculations have been performed for two symmetric isotopomers, 666 and 686, and one non-symmetric one, 668. The corresponding vibrational wave functions Φ_n for these three (non-rotating) isotopomers, required for expanding the scattering wave function, have been calculated by means of the filter diagonalization (FD) method.[17] **The same simplified PES, $V_{\rm mod}$, used in I, has been employed in these bound state calculations. It has been obtained by removing the three long-range van der Waals wells by exponential extrapolation along the dissociation coordinate from a value inside the main well to the correct asymptotic limit. In addition, two of the three main ozone potential wells have been eliminated by extrapolation along the bond angle α from $\alpha = 85°$ to 0. The extrapolations have been made so that $V_{\rm mod}$ and its first derivatives are continuous. Details are described in I.** The vibrational wave functions Φ_n are functions of the internal ozone coordinates: R, the distance of the central O atom to the center of mass of the two end O atoms; r, the distance between the two end atoms; and γ, the angle between R and r. (R, r, γ) form a set of Jacobi coordinates. The wave functions for symmetric isotopomers are either symmetric or anti-symmetric with respect to $\gamma = \pi/2$. All vibrational states up to the dissociation threshold — 244, 254, and 259 for 666, 668, and 686, respectively —- are considered in the scattering calculations.

In an attempt to model in a simple way the $O+O_2$ continuum we additionally calculated, by the FD method, wave functions of states with energies above the dissociation limit. An absorbing potential at the grid boundary was not used in these calculations, i.e., these real-valued so-called "box states" are zero at the grid boundary. They represent artificial bound states and extend the true bound states, to which they are orthogonal, into the continuum. The "box states" were calculated only for 666 (80 states) and 668 (90 states). They were not part of the main study, but included only in some test calculations.

The collision of Ar with O_3 is described by the polar coordinates ρ, θ, and φ defined with respect to a coordinate system, in which the center-of-mass of O_3 is the origin and O_3 lies in the XY plane with the central O atom located on the positive X axis.[18] According to this choice of coordinates, $\theta = 0$ represents Ar approaching perpendicular to the plane of O_3 (i.e., along the Z axis) and $\theta = 90°$ corresponds to in-plane collisions. For an in-plane collision, $\varphi = 0$ corresponds to Ar approaching along the X axis. The interaction potential $V_{\mathrm{Ar-O_3}}$ between the Ar atom and O_3 is written as a sum of three Ar−O potentials $V_{\mathrm{Ar-O}}(R_i)$, where R_1, R_2, and R_3 are the three $\mathrm{Ar}-\mathrm{O}$ distances.[9] The evaluation of $V_{\mathrm{Ar-O_3}}$ requires the determination of the R_i for a given set of scattering coordinates $(R, r, \gamma, \rho, \theta, \varphi)$. This is done using the condition that the angular momentum vector of ozone is zero.[18]

In the IOSA one has to solve an $\mathrm{Ar}-\mathrm{O_3}$ scattering problem for a set of fixed angles (θ, φ). The time-independent Schrödinger equation for the lth partial wave Ψ^l is given by

$$\left[-\frac{\hbar^2}{2\mu}\frac{\partial^2}{\partial\rho^2} + \frac{\hbar^2}{2\mu}\frac{l(l+1)}{\rho^2} + \hat{h}_{\mathrm{O_3}}(R, r, \gamma) + V_{\mathrm{Ar-O_3}}(R, r, \gamma, \rho, \theta, \varphi) - E\right]\Psi^l = 0\,, \qquad (1)$$

where the angles θ and φ enter only as parameters. Expanding Ψ^l in terms of the eigenfunctions $\Phi_n(R, r, \gamma)$ of $\hat{h}_{\mathrm{O_3}}$, one obtains the set of coupled equations,

$$\left(\frac{d^2}{d\rho^2} - \frac{l(l+1)}{\rho^2} + k_{n'}^2\right)\chi_{n'l}(\rho|\theta, \varphi) = \frac{2\mu}{\hbar^2}\sum_{n''} V_{n'n''}(\rho|\theta, \varphi)\chi_{n''l}(\rho|\theta, \varphi) \qquad (2)$$

for the angle dependent radial expansion functions $\chi_{n'l}(\rho|\theta, \varphi)$; $k_{n'}^2 = 2\mu(E - E_{n'})/\hbar^2$ and $E_{n'}$ and μ are the vibrational energies of ozone and the $\mathrm{Ar}-\mathrm{O_3}$ reduced mass, respectively.

The potential matrix elements are defined by[19]

$$V_{n'n''}(\rho|\theta, \varphi) = \int dR \int dr \int d\gamma \sin\gamma\, \Phi_{n'} V(R, r, \gamma, \rho, \theta, \varphi)\Phi_{n''}. \qquad (3)$$

The $\mathrm{Ar}-\mathrm{O_3}$ interaction potential is strongly anisotropic as illustrated in Fig. 1, which shows a selection of diagonal matrix elements $V_{nn}(\rho)$ for 686 for several pairs (θ, φ). The quantum

state is $n = 230$ with an energy of $213\,\mathrm{cm}^{-1}$ below the threshold. The approach perpendicular to the ozone plane ($\theta = 0$) allows the closest encounter between Ar and O_3. Approaching one of the end atoms in the plane spanned by O_3 leads to the strongest repulsion ($\varphi = 105°$ in Fig. 1). The nondiagonal coupling elements are also strongly angle dependent.

Solution of the coupled equations with the appropriate boundary conditions and summation over l yields vibrationally inelastic cross sections $\sigma_{n'n}(\theta, \varphi)$.[9] All quantum mechanical calculations presented below are for a collision energy of $E_c = 200\,\mathrm{cm}^{-1}$. The strong angle dependence of the $V_{n'n}$ implies a large anisotropy of the $\sigma_{n'n}(\theta, \varphi)$ illustrated in Fig. 2 for the sum of inelastic cross sections. The cross sections for the symmetric isotopomers are symmetric with respect to $\varphi = 180°$, while this symmetry does not exist for non-symmetric molecules. For $\theta = 0$ the cross sections are independent of φ. The sum of inelastic cross sections for the same initial state varies by more than two orders of magnitude over the full sphere. The inelasticity is generally weakest for the perpendicular approach.

The final cross sections are obtained by averaging over the angles,[19]

$$\sigma_{n'n} = (4\pi)^{-1} \int_0^{\pi} d\theta \sin\theta \int_0^{2\pi} d\varphi\, \sigma_{n'n}(\theta, \varphi)\,. \tag{4}$$

The highly oscillatory character of the $\sigma_{n'n}(\theta, \varphi)$ requires a dense grid for the numerical integration. The integration over θ involved the grid points $\theta_i = 90°$, $60°$, $45°$, $30°$, and 0; the cross sections are symmetric with respect to $90°$. The integration over φ used 24 equally spaced points $0 \le \varphi_j \le 345°$ with $\Delta\varphi = 15°$. For $\theta = 0$ only one angle φ is necessary. Thus, the total two-dimensional grid included 97 points for non-symmetric molecules. Because of the symmetry with respect to $\varphi = 180°$, the analogous grid for symmetric molecules contained only 53 points. The integration scheme used to evaluate Eq.(4) took into account the special character of the function $\sin\theta\,\sigma_{n'n}(\theta, \varphi)$ at $\theta = 0$ and $90°$: At $\theta = 0$ the function is zero and the first derivative with respect to θ is finite, whereas for $\theta = 90°$ the function is finite and the derivative is zero.

For comparison with data obtained in I and in the classical calculations we define transition probabilities according to

$$Q_{n'n} = \sigma_{n'n}/\sigma_0 \tag{5}$$

where σ_0 is a common cross section. In what follows we will use the value $\sigma_0 = 437.8\text{Å}^2$, which is the largest total cross section obtained in the BSA.[9] The main quantity considered

in this work is the collision induced vibrational energy transfer (first moment)

$$\Delta E_n = \sum_{n' \neq n} Q_{n'n}\, \Delta E_{n'n}\,, \tag{6}$$

where $\Delta E_{n'n} = E_{n'} - E_n$. An alternative quantity is the downward energy transfer $\Delta E_n^{(-)}$, for which the summation in Eq.(6) is limited to $n' < n$; it was the main term considered in I. Both ΔE_n and $\Delta E_n^{(-)}$ give qualitatively similar descriptions of the energy transfer in ozone.

B. Classical trajectory calculations

An obvious question is how the quantum mechanical energy transfer compares with the vibrational energy transfer obtained from classical trajectories. Details of the classical calculations are described elsewhere.[20,21] For consistency with the quantum mechanical calculations, the ozone molecule is prepared with zero total angular momentum and a specific internal energy $E_{\rm int}$ before the collision. Although O_3 initially does not rotate, during the collision it will be rotationally excited and the rotational energy transfer actually is about one order of magnitude larger than the vibrational energy transfer.[21] In order to compare with the quantum mechanical studies, which consider only vibrational energy exchange, the rotational and the vibrational contributions to the internal energy therefore were separated as described by Ivanov *et al.*[20] Briefly, the instantaneous tensor of inertia is diagonalized at each point on a trajectory and an instantaneous rotational energy $T_{\rm r}$ is defined using standard expressions. $T_{\rm r}$ is a highly oscillatory function of time. However, averaging over a time interval Δt and over an ensemble of many trajectories removes the oscillations, which allows to calculate the vibrational energy after the collision according to $E_{\rm int} - T_{\rm r}$. Because of intramolecular energy flow between the vibrational degrees of freedom, on one hand, and the 'active' rotational degrees of freedom, related to the projection quantum number K_a, on the other, the classical vibrational energy is not constant.[20] The rate of this intramolecular energy redistribution is an increasing function of K_a as well as the internal energy. However, on the collisional time scale of ~ 1 ps it can be neglected and a meaningful vibrational energy transfer $\Delta E_{\rm vib}^{\rm cl}$ can be extracted.

Calculations were performed for several internal energies of the isotopomers 686 and 668. For each energy between 0.5×10^6 and 1.0×10^6 trajectories were calculated. In all cases

the maximum impact parameter was set to $b_{\max} = 7$Å which corresponds to a cross section of $\pi b_{\max}^2 = 153.9$Å^2. This large impact parameter guarantees that $\Delta E_{\rm vib}^{\rm cl}$ is practically zero beyond $b_{\max}$. For comparison with the quantum mechanical ΔE_n, however, it is necessary to normalize $\Delta E_{\rm vib}^{\rm cl}$ to the same total cross section. Therefore, $\Delta E_{\rm vib}^{\rm cl}$ is multiplied with $\pi b_{\max}^2/\sigma_0 = 0.351$, where σ_0 is the cross section used in Eq.(5).

III. RESULTS

A. Vibrational energy transfer in a single collision

The vibrational energy transfer was calculated for all states up to the dissociation threshold for the isotopomers 666, 686, and 668. ΔE_n is negative for the majority of vibrational states in all three isotopomers; at a collision energy of 200 cm^{-1}, ozone is preferentially de-excited by argon. Despite averaging over many orientation angles, ΔE_n in the IOSA is strongly state-specific. The energy transfer fluctuates over two orders of magnitude, and the amplitude of fluctuations is comparable with that in the BSA (Ref. 9). These fluctuations reflect the individual nodal patterns of the vibrational eigenstates, which in ozone are even at high energies mostly assignable.[22] For the presentation, the fluctuations are smoothed by averaging ΔE_n over twenty neighboring states. [Throughout the following, ΔE_n will always represent the smoothed energy transfer without special notation.] The results for 686 and 668 are depicted in Fig. 3; the data for 666 are similar. In the figure, the IOSA results are compared with the (smoothed) BSA results of Ref. 9 and with the classical trajectory calculations. Despite the averaging the IOSA and BSA energy transfers still exhibit substantial fluctuations. They are slightly more pronounced for the symmetric molecule. The energy zero in Fig. 3 corresponds to the quantum mechanical thresholds in the IOSA and the BSA calculations.

We first discuss the quantum mechanical energy transfer in the 668 isotopomer. Surprisingly, the BSA and the IOSA results are close to each other near the dissociation threshold, where the deviation is smaller than a factor of two. However, the energy transfer in the IOSA is much less energy dependent than in the BSA: The slope of ΔE_n vs. E_n in the IOSA is substantially smaller than in the BSA over a broad energy range down to about -4000 cm^{-1}. This difference in slopes reflects inelastic energy exchange in different groups of vibrational

states. For the BSA, the demonstration of this relation was a focal point of I. The same analysis is directly applicable to the IOSA energy transfer in Fig. 3. As in I, we restrict the discussion to the most probable downward transitions $m(\max) \rightarrow n'(\max)$ which dominate the smoothed downward energy transfer, $\Delta E_n^{(-)}$; the downward energy transfer $\Delta E_n^{(-)}$, both in the IOSA and the BSA, has the same slope as ΔE_n. These transitions faithfully describe the exact energy transfer for internal ozone energies up to $E_n \leq -2000\,\mathrm{cm}^{-1}$, and it is this energy range, free from any boundary effects, which we are primarily concerned with. The algorithm to isolate the characteristic transitions $m(\max) \rightarrow n'(\max)$ has been described in detail in Ref. 9.

The most probable downward transitions in 668 are mapped onto the vibrational spectrum of ozone in Fig. 4. All states with $E_n \leq -2000\,\mathrm{cm}^{-1}$ can be assigned vibrational quantum numbers of the symmetric (n_s) and anti-symmetric (n_a) stretch and the bend (n_b). More relevant for ozone with its accidental 1:1 resonance between the symmetric and the anti-symmetric modes, however, is the assignment in terms of the polyad quantum number $\mathcal{P} = n_s + n_a$ and the bending quantum number n_b (Fig. 4). In the BSA and for energies $E_n \geq -4000\,\mathrm{cm}^{-1}$, transitions occur predominantly between states belonging to different polyads, $\Delta\mathcal{P} \neq 0$ [see Fig. 4(a) and Ref. 9]. The energies of these states are close to each other and are related via a set of resonance conditions which are satisfied by the vibrational frequencies as discussed in I. Below $-4000\,\mathrm{cm}^{-1}$, however, the transitions between adjacent states inside one polyad, $\Delta\mathcal{P} = 0$, become the most probable ones. These states are quasi-degenerate, too, because of the near-resonance of the symmetric and the anti-symmetric stretching frequencies. The transition from mainly inter-polyad to mainly intra-polyad energy transfer explains, according to I, the sharp change in the slope of ΔE_n vs E_n in the BSA around $-4000\,\mathrm{cm}^{-1}$ (black thin curve in Fig. 3). Inter-polyad transitions involving simultaneous change of all quantum numbers require higher order anharmonicities in the potential making its matrix elements strongly energy (or quantum number) dependent. In contrast, the intra-polyad transitions, involving merely an incremental change in n_a and n_s, give rise to the more gently declined branch of ΔE_n at lower energies.

The IOSA interaction drastically simplifies the pattern of most probable transitions in 668 [see Fig. 4(b)]. For all energies below $-2000\,\mathrm{cm}^{-1}$, the dominant transitions are exclusively those inside polyads. As a result, the slope of the IOSA energy transfer is consistently smaller than in the BSA for all energies $E_n \geq -4000\,\mathrm{cm}^{-1}$. Below $-4000\,\mathrm{cm}^{-1}$, where the

dominant transitions in both approximations occur inside polyads, the slope of the IOSA energy transfer is roughly equal to the slope of the BSA ΔE_n.

The drastic difference between the state-specific energy transfer dynamics in the two approximations becomes conspicuous in 666 (see Fig. 5). Each polyad in symmetric molecules consists of alternate symmetric and anti-symmetric states with even and odd n_a, respectively. The BSA is a symmetry preserving approximation: The corresponding $\mathrm{Ar} - \mathrm{O}_3$ potential is symmetric with respect to interchange of the two end oxygen atoms, and transitions between states of opposite symmetries are forbidden. Thus, all dominant transitions in the BSA are of the inter-polyad type [Fig. 5(a)]. As a consequence, the BSA energy transfer in 666 and likewise 686 is strongly energy dependent throughout the whole ozone spectrum (Fig. 3). Below $E_n = -4000\,\mathrm{cm}^{-1}$, this energy dependence gives rise to the pronounced symmetry effect discussed in I. The non-symmetric IOSA interaction reverses the energy transfer dynamics in 666: Symmetry-breaking intra-polyad transitions become dominant at all energies [Fig. 5(b)] and the slope of the IOSA energy transfer is much smaller than in the BSA.

Comparison of the IOSA results for 666 and 668 [cf. Fig. 4(b) and Fig. 5(b)] shows that the most probable downward energy flow is almost indistinguishable in both molecules. As a result, the smoothed IOSA energy transfers in the symmetric (666 and 686) and the non-symmetric (668) isotopomers are nearly equal to each other (Fig. 3).

A quantitative comparison between ΔE_n in the IOSA and in the BSA depends on the initial ozone energy. At low E_n, the energy transfer in the IOSA is about one order of magnitude larger than in the BSA. However, above $E_n = -4000\,\mathrm{cm}^{-1}$ the BSA ΔE_n increases more rapidly than the IOSA ΔE_n and the discrepancy gradually becomes less dramatic. At about $-1000\,\mathrm{cm}^{-1}$ the ratio is only two and becomes even smaller for energies closer to the threshold.

Both quantum mechanical approximations show a drastic increase of ΔE_n in the energy range about $200\,\mathrm{cm}^{-1}$ below threshold. This is an artifact of the calculations and originates from the restriction of the vibrational basis to bound states only. This was tested by calculations, for one partial wave l, in which the vibrational basis was augmented by the "box states": Extending the vibrational basis to energies above threshold removes the sharp increase of ΔE_n near $E_n \approx 0$. The results for other l values are expected to show the same changes when the basis is augmented and therefore we conclude that the l-averaged energy

transfer varies gradually near threshold — like the classical vibrational energy transfer.

The IOSA energy transfer agrees over a large range of internal energy very well with $\Delta E_{\rm vib}^{\rm cl}$ (Fig. 3). Especially the increase with E_n is satisfactorily reproduced by the classical calculations. The comparison between the quantum mechanical and the classical calculations is by no means trivial. First, for the classical results $E = 0$ corresponds to the classical dissociation threshold while for the quantum mechanical calculations it corresponds to the quantum mechanical threshold; the difference is of the order of $800\,{\rm cm}^{-1}$. Second, ozone is rotationally excited in the classical collisions and the 'active' rotational degrees of freedom are coupled to the vibrational motion. The pure vibrational energy transfer is very small and in the classical calculations it is obtained by subtracting two much larger quantities, $E_{\rm int}$ and $T_{\rm r}$. This may also be the origin of the relatively large difference between the results for 668 and 686 at very low energies ($E_n \approx -6000\,{\rm cm}^{-1}$). $\Delta E_{\rm vib}^{\rm cl}$ seems to exhibit a slight isotope effect: The result for the symmetric molecule is consistently larger than the energy transfer for the non-symmetric one. However, in view of the complexity of the classical calculations it is not justified to further dwell on this difference.

The agreement between the IOSA and the classical calculations is remarkable. We know only one other study in which the energy transfer from highly excited molecules has been calculated by quantum mechanical and classical methods: The collinear collision of CS_2 with He.[23] In that study, which because of lack of rotation is considerably simpler than three-dimensional $Ar + O_3$ collisions, also perfect agreement between the classical and the averaged quantum mechanical energy transfer has been found.

B. Vibrational energy transfer in multiple collisions

In I we additionally investigated vibrational relaxation of excited ozone via a master equation approach. In a simple finite difference form of the master equation on a discrete grid τ_k of the dimensionless time $\tau = \omega_0 t$ ($\tau_k - \tau_{k-1} = 1$) the change of the population of state n is calculated iteratively by

$$z_n(k+1) = \sum_{n'} Q_{nn'}\, z_{n'}(k) \tag{7}$$

("multiple collisions"). The non-diagonal elements $Q_{nn'}$ are defined in Eq.(5) and the diagonal elements are given by $Q_{nn} = 1 - \sum_{n' \neq n} Q_{n'n}$. In I, the probabilities were determined

for a fixed temperature by averaging over the collision energy E_c according to the Maxwell distribution. Because the IOSA calculations are considerably more time consuming, the $Q_{nn'}$ in the present work are calculated for a fixed collision energy $E_c = 200\,\mathrm{cm}^{-1}$. The initial distribution $z_n(0)$ includes a few of the uppermost states. Repetition of Eq.(7) results in the relaxation of the average energy $\bar{E}_k = \sum_n z_n(k) E_n$. The energy relaxation rate $\overline{\Delta E}_k = \bar{E}_k - \bar{E}_{k+1}$ is given by

$$\overline{\Delta E}_k = \sum_n z_n(k) \Delta E_n \,, \tag{8}$$

where ΔE_n is defined in Eq.(6).

In Fig. 6 we show $\overline{\Delta E}_k$ as function of the average ozone energy $\bar{E}_k$ for 668 and 686. According to Eq.(8), $\overline{\Delta E}_k$ is an average of the state specific energy transfer in a single collision with Ar. The weighting is provided by the actual populations $z_n(k)$, i.e., it is a 'dynamical' weighting. The results for the two isotopomers are basically identical. For comparison we also show the average state specific energy transfer ΔE_n obtained by averaging over 20 neighboring initial states. Except for energies above $-1500\,\mathrm{cm}^{-1}$ the energy transfer from the multiple collision approach, $\overline{\Delta E}_k$, is smaller than the average first moment ΔE_n. The deviations are largest at energies below $-4000\,\mathrm{cm}^{-1}$. The origin of the difference is the different weighting in the averaging process — dynamical weighting in the master equation approach vs. uniform weighting in the single collision procedure — and has been analyzed in I.

C. Simple stabilization/dissociation model

We used the discretized master equation, Eq.(7), to mimic in a simple way the stabilization and dissociation of highly excited ozone molecules. If Ar collides with ozone molecules in vibrational states close to the dissociation threshold, some fraction of molecules will be de-excited and the remaining part will be excited into the continuum. In the simple model we assume that the molecules excited to continuum states will immediately dissociate — i.e., their population is set to zero in the next iteration — and therefore the percentage of stable molecules, $P_{\mathrm{stab}}(k) = \sum_n z_n(k)$, gradually decreases with k; the sum extends over all bound states. In the limit of large k, $P_{\mathrm{stab}}(k)$ approaches a constant value and we define this constant as the stabilization probability P_{stab}. It depends on the particular initial state n. The association of O and O_2 to form highly excited O_3, i.e., the first step of the Lindemann

mechanism, is not considered.

The most important question concerns the definition of continuum states. We performed two types of calculations. In the first approach we define all bound states above $-200\,\mathrm{cm}^{-1}$ as continuum states; in these calculations the cross section based probabilities $Q_{n'n}$ (summation over all partial waves, averaging over the full sphere) are used in Eq.(7). In the second set of calculations the "box states" above the dissociation threshold are considered as continuum, while all bound states are considered to represent stable ozone molecules. In the latter calculations only the transition probabilities for partial wave $l = 40$, averaged over φ for fixed $\theta = 90°$ (in-plane scattering), are considered in Eq.(7).

The stabilization probabilities for the various initial states n obtained in the two calculations are shown vs. E_n in Fig. 7. P_{stab} is very small for states close to the 'threshold' and then gradually rises towards one as the initial energy decreases. Molecules starting with an energy of a few hundred cm^{-1} below threshold are all stabilized. The energy at which P_{stab} starts to deviate from one depends, of course, on the collision energy. It also depends on the partial wave l, because the inelasticity and therefore the energy transfer depend on l.

The main result of these calculations is that the stabilization probability is independent of the symmetry of the isotopomer: Within the IOSA and the simple stabilization model, symmetric and non-symmetric isotopomers are stabilized with the same probability. Without showing results we note that the same finding is also obtained when the transition probabilities are calculated in the BSA. This is in accord with the energy transfer per collision, $\overline{\Delta E}_k$, being independent of symmetry in the upper energy regime $E_n > -1500\,\mathrm{cm}^{-1}$ or so.[9]

IV. SUMMARY

The state-resolved vibrational energy transfer ΔE_n in $\mathrm{Ar} - \mathrm{O}_3$ collisions has been investigated by means of the quantum mechanical infinite order sudden approximation (IOSA). The study complements our earlier investigation using the computationally much less laborious breathing sphere approximation (BSA).[9] At low ozone energies the IOSA ΔE_n is considerably larger than the energy transfer calculated with the BSA; the ratio is about one order of magnitude. Since the BSA energy transfer increases with E_n more rapidly than the IOSA ΔE_n, the disparity becomes less significant with increasing E_n. Around the threshold both approximations predict almost the same vibrational energy transfer. The IOSA results

agree well with the vibrational energy transfer calculated by classical trajectories over the entire range of internal energies. Within this range, the vibrational energy transfer varies by more than an order of magnitude. To our knowledge, this is the first comparison of quantum mechanical and classical vibrational energy transfer in full-dimensional collisions of a highly excited polyatomic molecule with an atom.

The results for two isotopomers, 686 and 668, have been compared. Within the fluctuations of the averaged state specific ΔE_n the results for the symmetric and the non-symmetric isotopomers are essentially the same. This is valid for the IOSA, which does not conserve symmetry, for the entire range of E_n and it applies, at least for high energies, also to the BSA, which conserves symmetry. The pronounced symmetry effect found in the BSA at low ozone energies[9] is not relevant for the stabilization of highly excited ozone. Thus, we conclude that the vibrational energy transfer in collisions of highly excited O_3 with Ar does not depend on the symmetry of the isotopomer, at least not when ozone is treated as a simplified C_{2v} molecule. In cannot be precluded that the results may be different, when all the three main potential wells and the three van der Waals wells are taken into account; but that requires much more demanding calculations.

The stabilization process has been modeled with a simplified version of the discretized master equation, in which all states above a certain energy are considered to immediately dissociate. In accord with the independence of the energy transfer on the symmetry of ozone, the stabilization probabilities for the symmetric and the non-symmetric molecules are essentially the same.

Acknowledgments

Financial support by the Deutsche Forschungsgemeinschaft is gratefully acknowledged. The authors are grateful to S. Yu. Grebenshchikov for invaluable discussions and contributions. Especially the analysis of the energy transfer in terms of the polyad structure of the ozone spectrum in Sect. III.A and the related Figs. 4 and 5 are his work. To the regret of

the authors he could not be persuaded to co-author this article.

[1] K. Mauersberger, D. Krankowsky, C. Janssen and R. Schinke, Adv. At. Mol. Opt. Physics **50**, 1 (2005).

[2] R. Schinke, S. Yu. Grebenshchikov, M. V. Ivanov and P. Fleurat-Lessard, Annu. Rev. Phys. Chem. **57**, 625 (2006).

[3] C. Janssen, J. Guenther, K. Mauersberger and D. Krankowsky, Phys. Chem. Chem. Phys. **3**, 4718 (2001).

[4] Y. Q. Gao and R. A. Marcus, J. Chem. Phys. **116**, 137 (2002).

[5] R. Schinke and P. Fleurat-Lessard, J. Chem. Phys. **122**, 094317 (2005).

[6] S. Yu. Grebenshchikov, Few-Body Syst. **45**, 241 (2009).

[7] Y. Q. Gao and R. A. Marcus, Science **293**, 259 (2001).

[8] B. C. Hathorn and R. A. Marcus, J. Chem. Phys. **113**, 9497 (2000).

[9] M. V. Ivanov, S. Yu. Grebenshchikov and R. Schinke, J. Chem. Phys. **130**, 174311 (2009).

[10] D. C. Clary and G. Drolshagen, Chem. Phys. Lett. **81**, 21 (1981).

[11] G. A. Parker and R. T. Pack, J. Chem. Phys. **68**, 1585 (1978).

[12] R. Schinke and P. McGuire, Chem. Phys. **31**, 391 (1978).

[13] D. C. Clary, J. Chem. Phys. **75**, 209 (1981).

[14] D. Secrest, J. Chem. Phys. **62**, 710 (1975).

[15] D. Charlo and D. C. Clary, J. Chem. Phys. **120**, 2700 (2004).

[16] T. Xie and J. M. Bowman, Chem. Phys. Lett. **412**, 131 (2005).

[17] T. P. Grozdanov, V. A. Mandelshtam and H. S. Taylor, J. Chem. Phys. **103**, 7990 (1995).

[18] D. Charlo and D. C. Clary, J. Chem. Phys. **117**, 1660 (2002).

[19] Unfortunately, the correct volume elements have been neglected by mistake in the integrals in Eqs.(9) and (12) in Ref. 9. In the actual calculations, however, they have been taken into account.

[20] M. V. Ivanov, S. Yu. Grebenshchikov and R. Schinke, J. Chem. Phys. **120**, 10015 (2004).

[21] M. V. Ivanov and R. Schinke, J. Chem. Phys. **122**, 234318 (2005).

[22] R. Siebert, P. Fleurat-Lessard, R. Schinke, M. Bittererová and S. C. Farantos, J. Chem. Phys. **116**, 9749 (2002).

[23] C. G. Schatz and G. Lendvay, J. Chem. Phys. **106**, 3548 (1997).

FIG. 1: Elastic potential matrix elements $V_{nn}(\rho)$ for state $n = 230$ of isotopomer 686 and several angles (θ, φ). The innermost curve is for $\theta = 0°$ (perpendicular approach) while the other curves are for $\theta = 90°$ (in-plane collisions): $\varphi = 30°$ (inner curve), 180° (middle curve), and 105° (outer curve).

FIG. 2: Sum of angle-dependent inelastic cross sections, $\sum_{n' \neq n} \sigma_{n'n}(\theta, \varphi)$, as function of φ for different θ. □: 668, $\theta = 90°$; ■: 686, $\theta = 90°$; ●: 686, $\theta = 45°$; ▲: 686, $\theta = 30°$; dashed line: 686, $\theta = 0$. The initial states are $n = 225$ for 668 and $n = 230$ for 686.

FIG. 3: Comparison of the averaged state specific energy transfer ΔE_n vs. internal energy E as obtained from the IOSA and the BSA. Black: non-symmetric 668; red: symmetric 686. The symbols represent the corresponding classical trajectory results: ○ 668; ● 686.

FIG. 4: Energy levels of 668 grouped into polyads with fixed polyad quantum number $\mathcal{P} = n_s + n_a$. Each polyad contains $\mathcal{P} + 1$ levels, with the highest level always having $n_a = 0$. Black (gray) symbols correspond to states with even (odd) n_a. Numbers $0, 1, 2...$ in each stack of polyads denote the bending excitations n_b. The states to the right of the vertical dashed line ($\mathcal{P} > 4$) are not explicitly assigned. The arrows identify the most probable inelastic transitions $m(\max) \rightarrow n'(\max)$ in a single collision: (a) in the breathing sphere approximation; (b) in the infinite order sudden approximation. Energy (in cm^{-1}) is measured with respect to the lowest quantum mechanical dissociation threshold.

FIG. 5: Energy levels of 666 grouped into polyads with fixed polyad quantum number $\mathcal{P} = n_s + n_a$. Each polyad contains $\mathcal{P} + 1$ levels, with the highest level always having $n_a = 0$. Solid (open) symbols correspond to symmetric (anti-symmetric) states. Numbers $0, 1, 2...$ in each stack of polyads denote the bending excitations n_b. The arrows identify the most probable inelastic transitions $m(\max) \rightarrow n'(\max)$ in a single collision: (a) in the breathing sphere approximation; (b) in the infinite order sudden approximation. Energy (in cm^{-1}) is measured with respect to the lowest quantum mechanical dissociation threshold.

FIG. 6: Energy relaxation rate $\overline{\Delta E}_k$, Eq.(8), vs. ozone energy E obtained from the discretized master equation compared to the averaged energy transfer ΔE_n derived from single collisions.

FIG. 7: Stabilization probability P_{stab} vs. ozone energy. (a) Calculations with all bound states above $-200\,\mathrm{cm}^{-1}$ considered as continuum states; the vertical dashed line indicates the fictitious threshold. (b) Calculations including "box states" in order to simulate the continuum. Further details are given in the text.

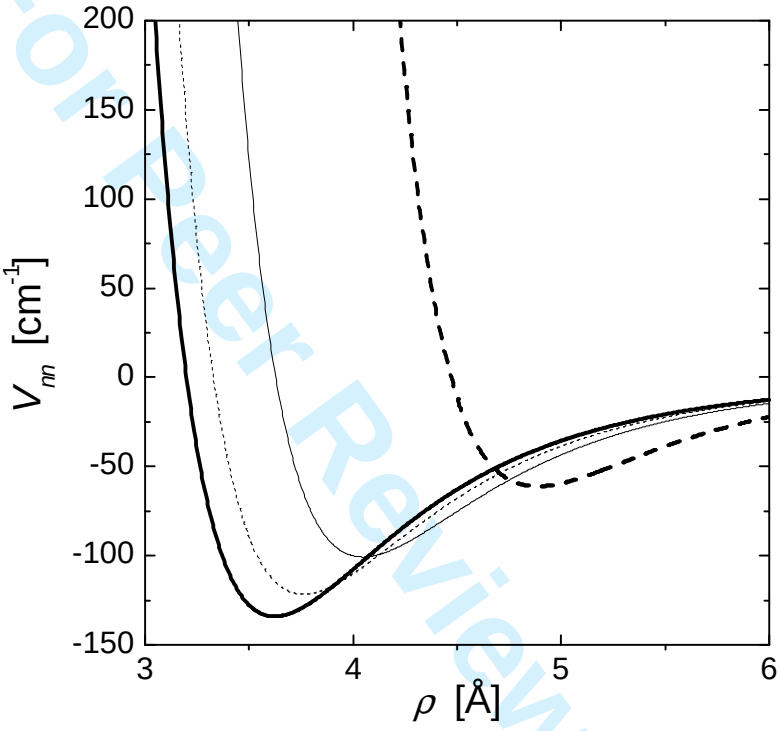

Fig. 1

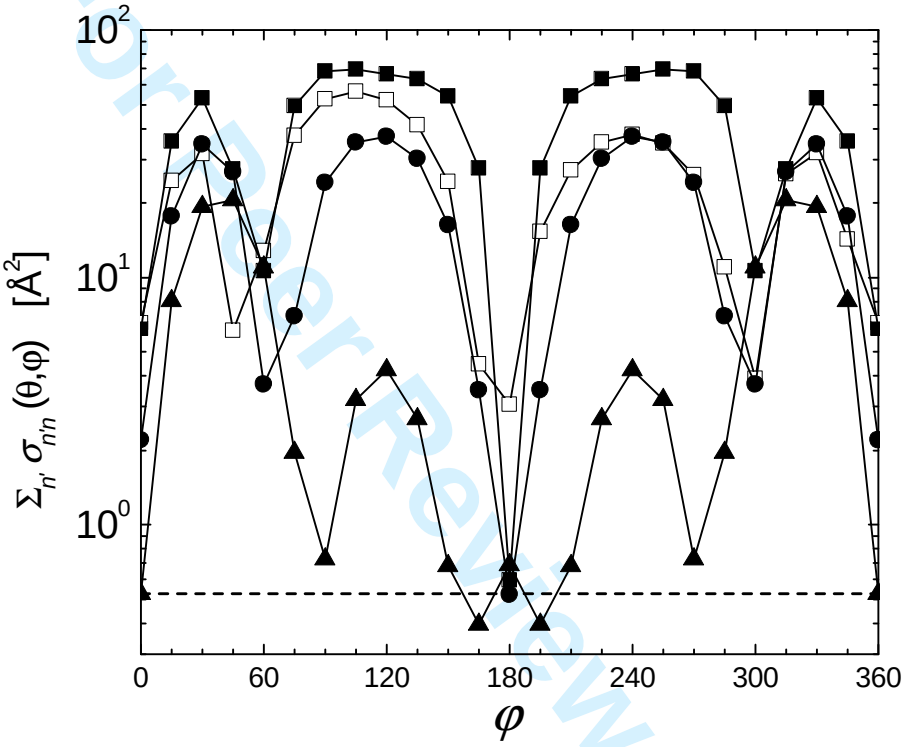

Fig. 2

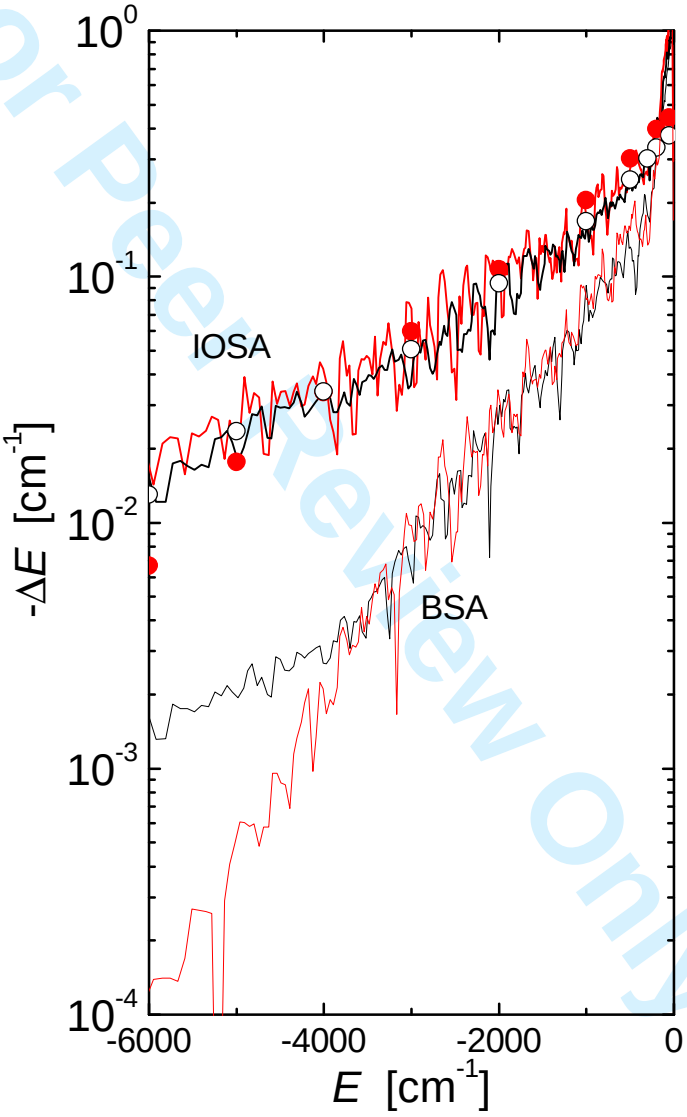

Fig. 3

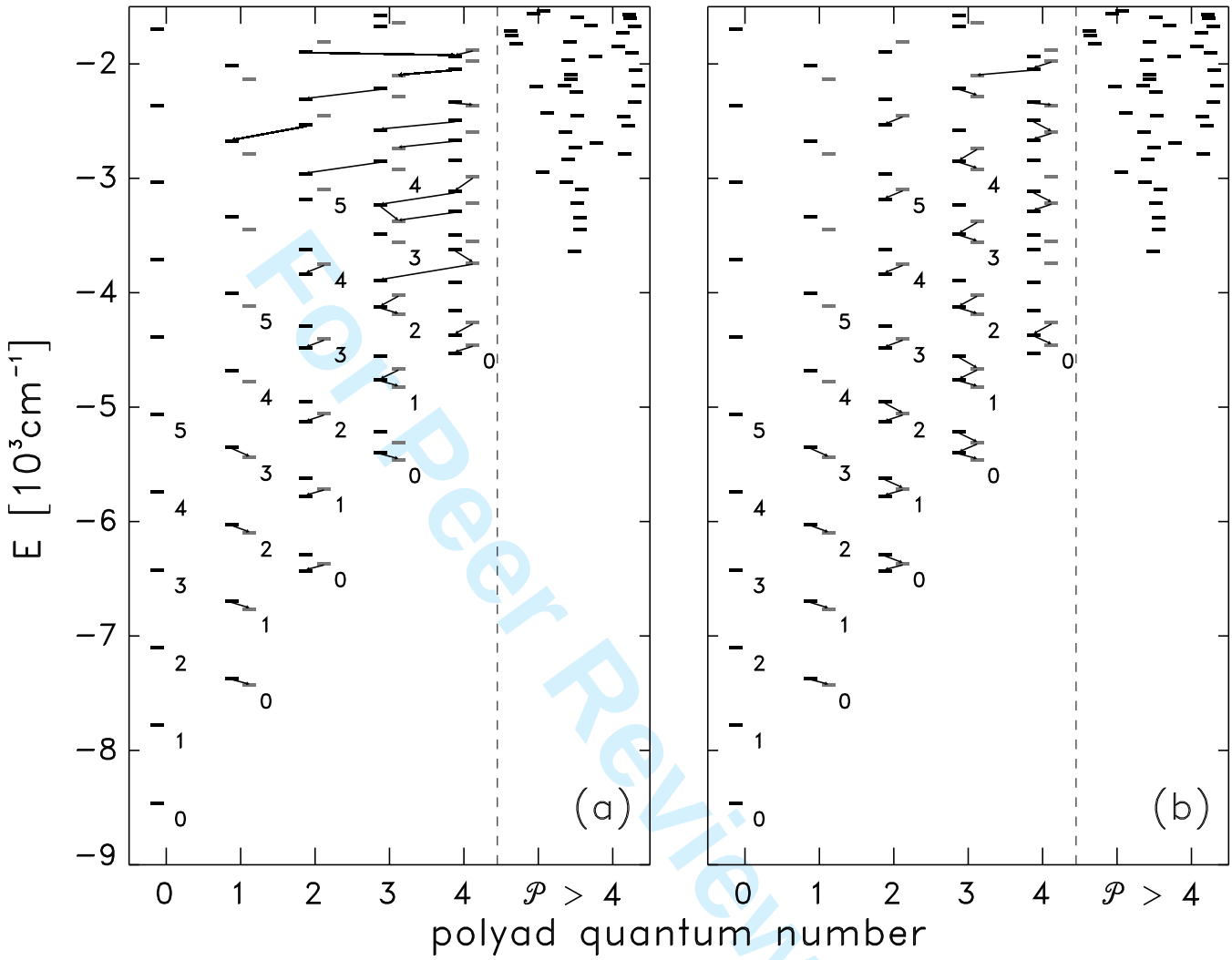

Fig. 4

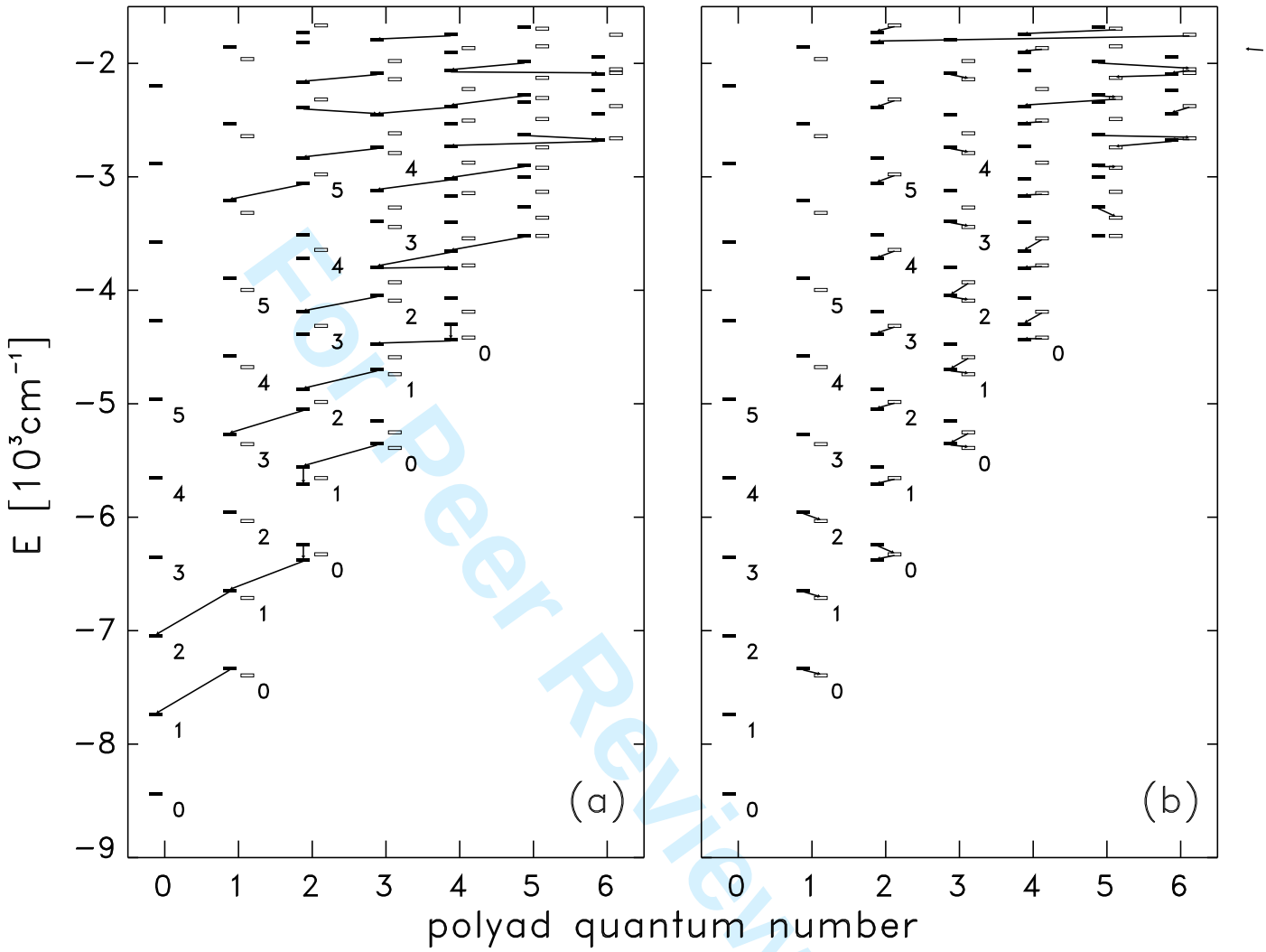

Fig. 5

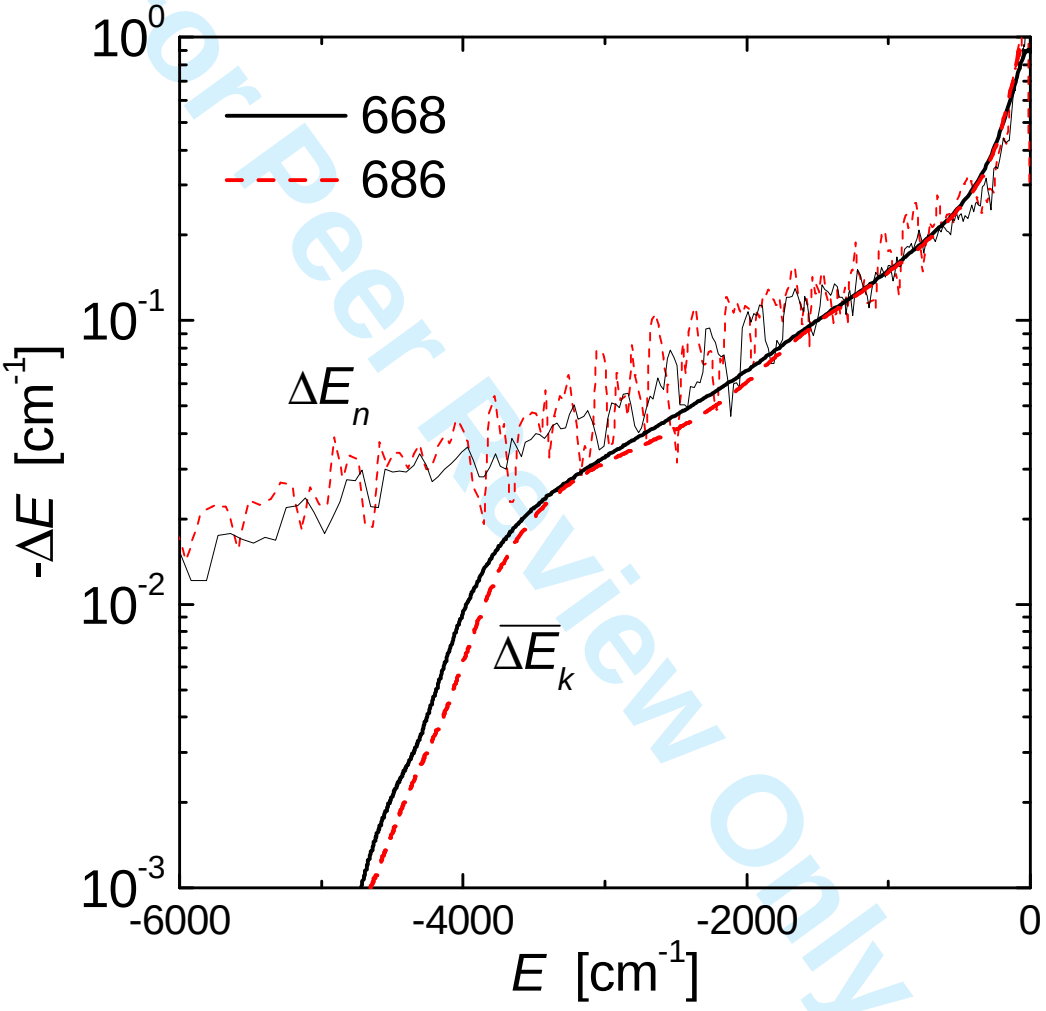

Fig. 6

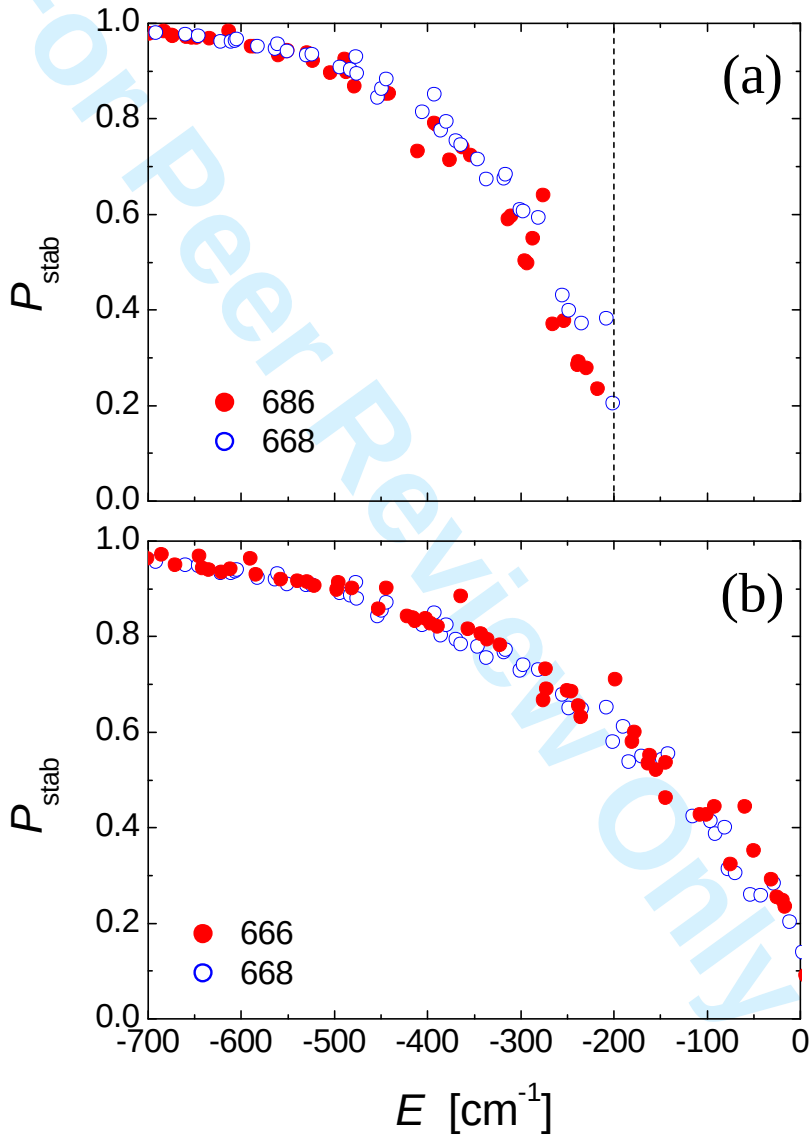

Fig. 7